A Low Cost Patternable Packaging Technology for Biosensors

A Low Cost Patternable Packaging Technology for Biosensors

Anthony Buchoux, Ewen O. Blair, Andreas Tsiamis, Jamie R. K. Marland and Stewart Smith
School of Engineering, The University of Edinburgh
SMC, Alexander Crum Brown Road,
Edinburgh, EH9 3FF, UK
Stewart.Smith@ed.ac.uk

***Abstract*—This paper demonstrates a simple and low cost technology to reliably and accurately package integrated chips. Microchannels and cavities of minimum feature size of 500 µm can be reliably reproduced. In addition, the curing depth in relation to the exposure time was investigated. A simple microfluidic device, consisting of a 500 µm channel and 2 mm ports, was manufactured to demonstrate the possibilities of this technology. Extensive electrochemical experiments showed that the packaging material is a good insulator and leaves no residue on the chip.**

Keywords— Biosensors; packaging; electrochemistry.

I. INTRODUCTION

The development of biomedical sensors based on integrated circuits requires packaging solutions which can protect electrical connections, such as gold wire-bonds, from an environment typically characterised by the presence of aqueous ionic solutions [1], [2]. At the same time, the sensor is likely to require direct contact with the solution, for example to allow a biosensor to interact with a specific biochemical in the environment. Therefore, there is a requirement to selectively provide mechanical and chemical protection to different parts of the device. This can be challenging to achieve in a simple and economical manner, especially as sensing systems have varied applications that tend to require complex and specific packaging solutions [3]–[7]. This includes the requirement for lab-on-a-chip style systems to have channels and inlets for microfluidic applications [8], [9]. There is a particular need for low-cost packaging for biosensors, so that point-of-care diagnostics are easily accessible to anyone [2], [10].

A popular method of patterning insulation layers involves selective exposure of photo-sensitive materials to ultra-violet light [11]–[12]. Video projectors using the Digital Light Processing (DLP) technology from Texas Instruments have been used by enthusiasts for photolithographic processes and as a source of light to selectively cure acrylic resins for DIY 3D printers. These projectors offer a route to efficiently and accurately package sensors at low cost using UV-curable acrylic resin.

This paper presents a system for the packaging of biosensors based on a DLP projector. The sensor chip is coated with UV-curable resin and the digital projector projects an image onto the surface. This selectively exposes certain areas of the resin to UV light, curing it to a solid. The areas not exposed remain liquid and can be removed with a suitable solvent such as isopropyl alcohol. This system yields several advantages: it is relatively low-cost to build (~£500), simple to assemble, easy to use, and versatile. The majority of the cost is taken up by the DLP projector itself, which could be substituted for a cheaper model to lower the price. The system is first described and the minimum feature size and curing properties are then characterised. The ability to use the packaging system to create fully enclosed channels and inlets, suitable for microfluidic systems is also demonstrated. Dedicated test structures (previously described in [13]) are then used to characterise the following aspects of the performance of packaging processes:

- presence of residual resin on the sensing surface after packaging,
- the stability of wire bonds during the process,
- the effectiveness of the chosen resin as an insulator, and
- monitoring of liquid ingress between the resin and chip

Finally, an electrochemical sensor is packaged and an exemplar measurement is made to confirm the operation of the system.

II. THE PACKAGING SYSTEM

A. Projector Setup

Fig. 1 (a) is a photograph of the packaging system set up, which includes a DLP projector (Acer, H6510BD, Acer inc., Taiwan) as a UV-light source. The light is focused onto an XY-stage, where the chip to be packaged is mounted. A laser-cut wooden frame is used to hold these components in place and provide structural support. The video projector has a resolution of 1920×1080 pixels, and the projection area at a typical working distance is 67.2×37.8 mm, giving an effective pixel size of 35 µm.

A graphical user interface (GUI) was developed in Matlab (MathWorks, Natick, Massachusetts, USA) to control the system. This interface is shown in figure 1 (b), with the input parameters being the dimensions of the chip as well as the width of the four borders that can be covered with resin. Alternatively, image files can also be used as an input. Hence, the desired pattern can be drawn in a graphics program and projected onto the resin. This enables a wide variety of patterns to be quickly and easily created to suit the desired packaging requirements. The final parameter is the exposure time, defining how long the resin is exposed to UV light. By varying this parameter, and via

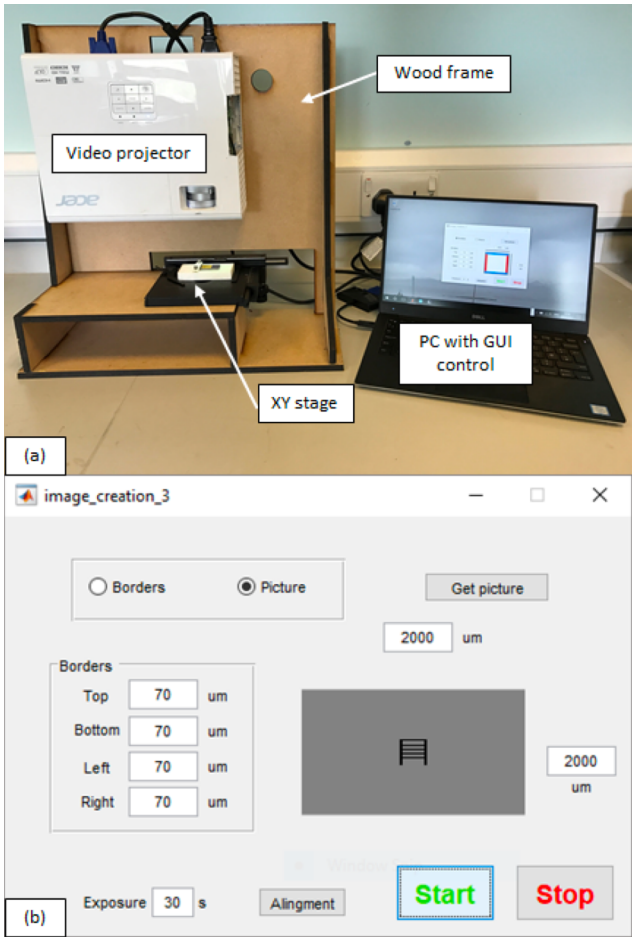

Fig. 1. (a) Packaging system setup with the laser-cut wooden frame supporting the video projector and the XY stage as well as the PC for control, (b) Graphical user interface to define and control the packaging process.

multiple exposures, the thickness of resin can be controlled to create cavities.

B. Packaging Process

To package a sensor, the chip is bonded into a dual in-line package, which is placed on the XY stage and the length and width of the chip are entered into the software. Alignment is achieved by using the "chip alignment" feature, which projects a box of white light onto the stage with the same dimensions as the chip. The chip can then be moved to line up with the projected image and the alignment tolerance is defined by the stepping resolution of the XY-stage. The package is then filled with acrylic resin (Spot – GP, Spot – A Materials, Spain) using a pipette. The pattern to be projected onto the chip is then entered, the exposure time is set, and the resin is exposed. Finally, after exposure, the uncured resin is removed with isopropyl alcohol and the chip is washed with deionised water.

III. System Characterisation

A. Dimensional Fidelity

To characterise the resolution of the system, test patterns were designed as shown in Fig. 2 (a) and (b). They consist of:

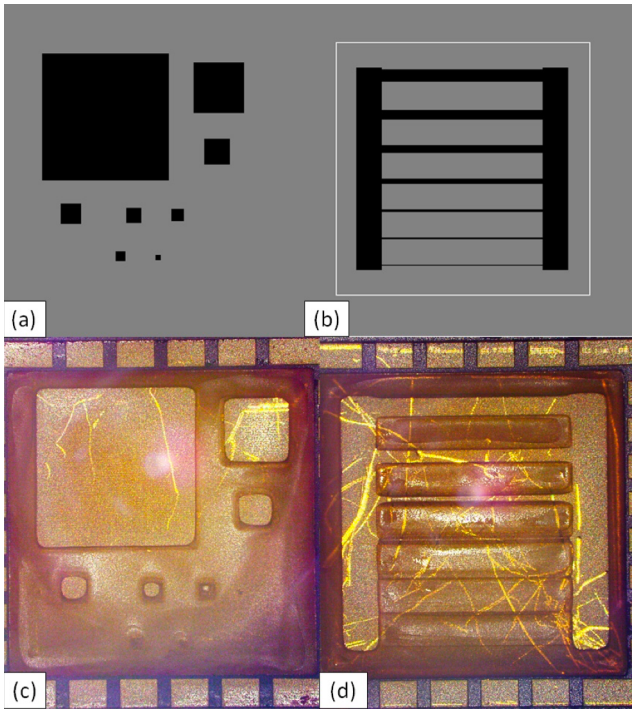

Fig. 2. (a) Pattern designed to test feature size and accuracy, the squares range from 5 mm to 0.2 mm (b) Pattern design to test the minimum channel width that can be manufactured, from 500 µm to 35 µm (c) Pattern shown in (a) once exposed for 35 s and cleaned in IPA, the depth of the structures is 190 µm and (d) Pattern shown in (b) once exposed for 35 s and cleaned in IPA, the depth of the channels is 290 µm.

1. a series of consecutively smaller squares from ranging from 5000 µm down to 200 µm in edge length, which informs:
   a. the minimum resolution where well defined corners can be resolved, and
   b. the smallest shape that can be patterned
2. a series of channels of decreasing widths, ranging from 500 µm down to 35 µm, to test the aspect ratio.

The dimensions are rounded to the nearest multiple of 35 µm, which is the effective pixel size of the device, to increase sharpness and prevent blurry edges. The nominal dimensions and the measured values can be found in tables I and II. The black areas represent the surfaces that should remain exposed to the surroundings while the grey areas represent the parts where the resin will be cured. A grey scale image is used to reduce the luminosity of the video projector thus reducing the curing speed and assuring a better control of the process.

These patterns are directly related to potential applications, as having higher definition enables large numbers of more densely packed sensors to be packaged. The potential to cheaply and easily create microchannels would also be of great benefit.

Fig. 2 (c) and (d) presents optical microscopy images (Leica DM12000 M) of the resin after being patterned, with the designed test features. The dimensions of the test shapes projected onto the resin and the dimensions of the resultant

TABLE I. RESULTS FOR THE MINIMUM FEATURE SIZE EXPERIMENT.

Designed (µm)	Height (µm)	Width (µm)	Average (µm)	Difference (%)
5005	5136	5137	5136.5	2.6
1995	2117	2118	2117.5	6.1
1015	995	1057	1026	1.1
805	719	810	764.5	5.0
595	441	513	477	19.8
490	234	276	255	48.0
385	-	-	-	-
210	-	-	-	-

TABLE II. MEASUREMENTS TO DETERMINE THE SMALLEST CHANNEL THAT CAN BE MANUFACTURED.

Designed (µm)	490	385	315	140	105	70	35
Measured (µm)	572	377	162 - 191	42	-	-	-

shapes after curing are presented in tables I and II, along with the percentage difference. The smallest pattern that could be resolved was the 595 µm square, with an error of 19.8%; smaller patterns were partially or fully filled with cured resin. The minimum pattern size which was resolved with accurate dimensions was the 805 µm square, with an error of 5%. The minimum channel width achieved, varied from 162 to 191 µm although it was designed to be 315 µm, indicating overexposure. Larger channels were measured to be closer to their designed width while smaller channels were not developed.

B. Curing Characterisation

The rate of curing was also characterised, using the jig shown in Fig. 3 (a). The jig was 3D printed with a uPrint SE (Stratasys, Eden Prairie, USA) using acrylonitrile Butadiene Styrene (ABS). It has six recesses on the surface, starting at a depth of 0.25 mm and becoming deeper by 0.25 mm until the deepest one of 1.5 mm. One recess was filled with resin and the block exposed for an arbitrary period of time. If the resin cured through, then the recess was cleaned and the exposure time reduced by 1 second, until the resin did not fully cured, then the previous value is noted. If the resin did not fully cured, the same procedure was applied but instead 1 second of exposure was added. The experiment was repeated until the resin cured all the way through, then the time recorded. The procedure was performed twice for each cavity. The thickness of resin cured against time is shown in Fig. 3 (b).

This information is required in order to produce enclosed microfluidic channels over the surface of a chip. This can be done in a two stage process. First curing the full thickness of the applied resin to produce the channel walls and then applying a shorter exposure to the fresh resin. This cures from the surface first, leaving unexposed resin underneath which can be removed to leave a hollow microchannel. Fig. 4 shows a simple

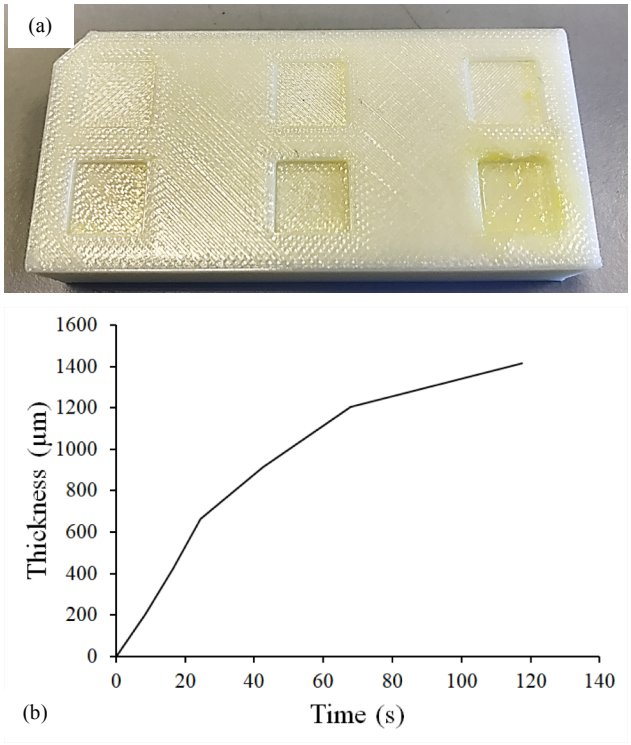

Fig. 3. (a) 3D printed test workpiece used to determine the curing rate for different thicknesses of resin. (b) Results of experiments showing the cured resin thickness against exposure time.

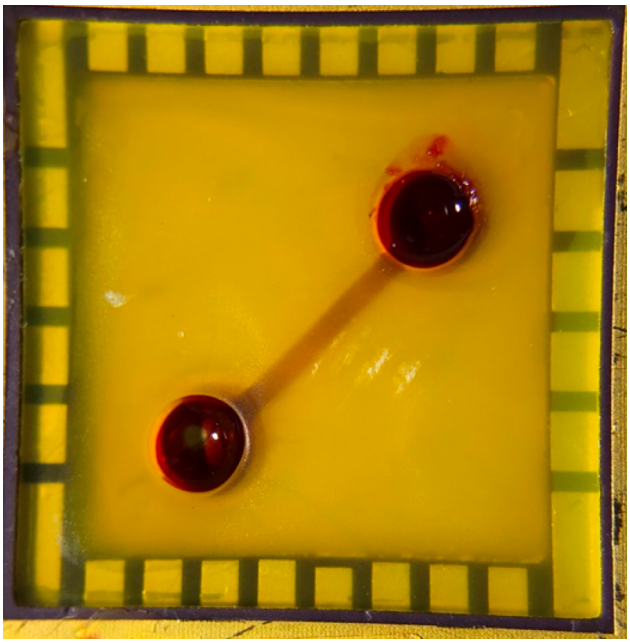

Fig. 4. Simple microfluidic device created via double exposure. A first layer of resin is exposed creating the channel and the wells, then a second layer is exposed with only the wells being patterned, covering the channel. Careful exposure timing, based on results from figure 3 a) ensures the resin is not cured through, creating the microfluidic device. Two 2 mm wells are connected via a 500 µm wide, 190 µm high and 5 mm long microchannel.

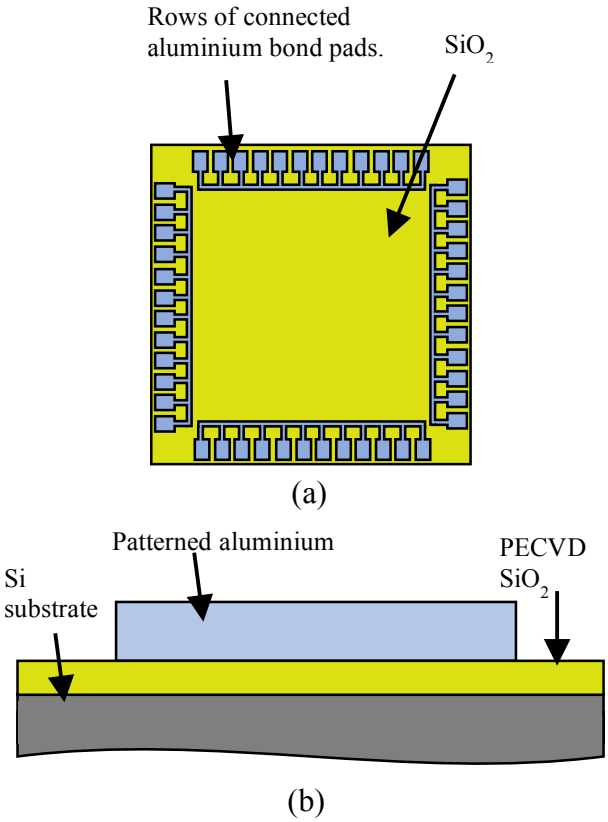

Fig. 5. (a) Schematic of the test structure used to characterise the packaging process and (b) a cross section through the test structure showing the layers

microfluidic device made of two 2 mm ports connected by a 0.5 mm wide channel. The first layer was exposed for 35 s then the excess resin was washed with IPA (the first layer is marginally over exposed to promote adhesion to the bottom of the package without reducing the process accuracy). Additional resin was pipetted in the package and exposed for 45 s to create the microchannel and the ports.

IV. Packaging Characterisation

A. Test Structures

Test structures were employed to assess the ability of the resin to function as a packaging material. This design was one of a series of test structures, dedicated to assessing packaging material properties, described elsewhere [12]. A schematic and a cross section of the test structure is presented in Fig. 5 (a) and (b) respectively. The test structure comprises four rows of interconnected aluminium bond pads along the edges of a 3x3mm square silicon chip, insulated with 500 nm of Plasma Enhanced Chemical Vapour Deposition (PECVD) SiO_2. This structure assesses the packaging process in three ways:

1. Monitoring stability of the wire bonds
2. Checking for the presence of residue left after the removal of uncured material
3. Quantifying leakage current, and hence the resin's effectiveness as an insulator

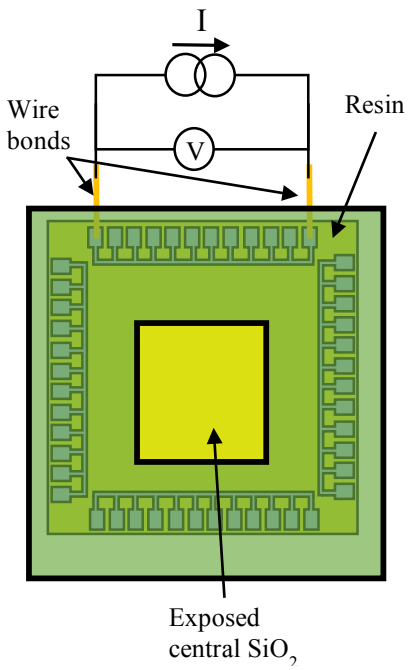

Fig. 6. Schematic of the two-terminal measurement being employed on the test structure to monitor connectivity of the wire bonds.

After gluing and wire bonding the chip into a ceramic package, the cavity was filled with resin and a 2 mm square window was patterned in the centre of the chip, exposing the central SiO_2 while insulating the wire bonds and aluminium bond pads.

The electrical connections were measured before dispensing the resin and after removing the uncured material. A schematic of the electrical path assessed is presented in Fig. 6. The resistances are shown in table III.

Damage to the wire bonds could occur through physical damage while dispensing the resin or shrinkage of the resin during the curing step, however the presence of a low resistance electrical path suggests the bond wires are undamaged by the packaging process.

A reflectometer was used to measure the thickness of the exposed central SiO_2. If any residue from the uncured resin remained, the measurement would be distorted. Table IV presents the average measured thickness of the SiO_2 before dispensing the resin and after removing the uncured material.

The insulation of the resin is electrochemically measured by filling the exposed cavity with KCl solution. A voltage was applied between the aluminium bond pads and a platinum electrode, dipped into the electrolyte, and the leakage current was monitored. A DC potential of +5 V was applied to the insulated electrode for 5 minutes and the measured current is presented in Fig. 7. The current measured is on the order of 10s of picoamperes and suggest that (a) there are no pinholes present in the resin and (b) there was no ingress of liquid at the resin/chip interface over the course of the measurement. Further

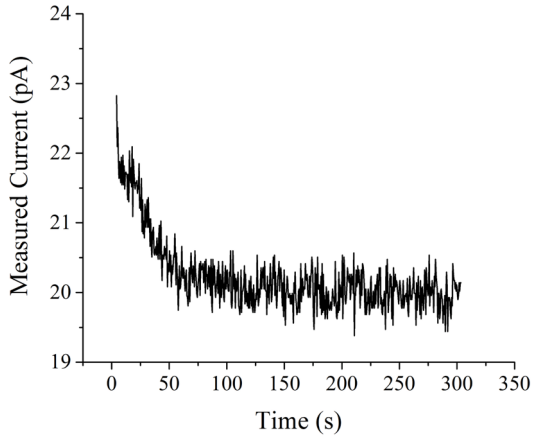

Fig. 7. Leakage current measured using the test structure presented in figure 5, packaged in resin. 5 V DC was applied for five minutes and the current was sampled every 0.5 seconds giving 601 points.

characterisation will be targeted at establishing the lifetime of the resin insulation.

V. Packaging an Electrochemical Sensor

Finally, a 3 x 3mm chip, with three on-chip electrodes was packaged and an exemplar measurement made, to demonstrate the feasibility of the system to package an electrochemical sensor. A chip with a platinum microelectrode was chosen as a sensing electrode, because the measured limiting current (i_L) from an electrochemical reaction at a microelectrode can be theoretically predicted. This afforded the opportunity to validate the packaging system.

Fig. 8 shows an optical image of the sensor chip, which consists of a three platinum electrodes: (a) a 5 µm radius disc working electrode, (b) a 5892 µm^2 area platinum pseudo-reference electrode, and (c) a 19641 µm^2 area platinum counter electrode. The chip was wire bonded into a ceramic package and packaged using the process described above, exposing a 2.25 mm^2 square window over the electrodes. Measurements were made in a Faraday cage using a PGSTAT12 potentiostat (Metrohm, Utrecht, Netherlands), against the on-chip platinum reference electrode. The working electrode was cleaned in 500 mM KCl by sweeping the potential between the solvent limits (at which water is electrolysed) for 20 minutes in a droplet of solution, pipetted onto the surface of the package over the exposed electrodes.

The reduction of ferricyanide to ferrocyanide was then used as a benchmark redox reaction and was measured in the same manner. Fig. 9 shows a cyclic voltammogram recorded in 1.2 mM of potassium ferricyanide in 500 mM KCl background electrolyte at 200 mVs^{-1}. The expected limiting current at a microelectrode can be calculated using

$$i_L = 4DcnrF \quad (1)$$

where D and c are the diffusion coefficient and concentration the of ferricyanide respectively, n is the number of electrons transferred in the reaction, r is the radius of the electrode, and F is the Faraday constant. Using a literature value for D of 0.667×10^{-5}cm^{2}s^{-1} from [14], a value of 1.54 nA was calculated. This matches the average measured value of 1.52 ± 0.06 nA, taken from five measurements. It is gratifying that the electrodes packaged with the system presented in this paper function as expected.

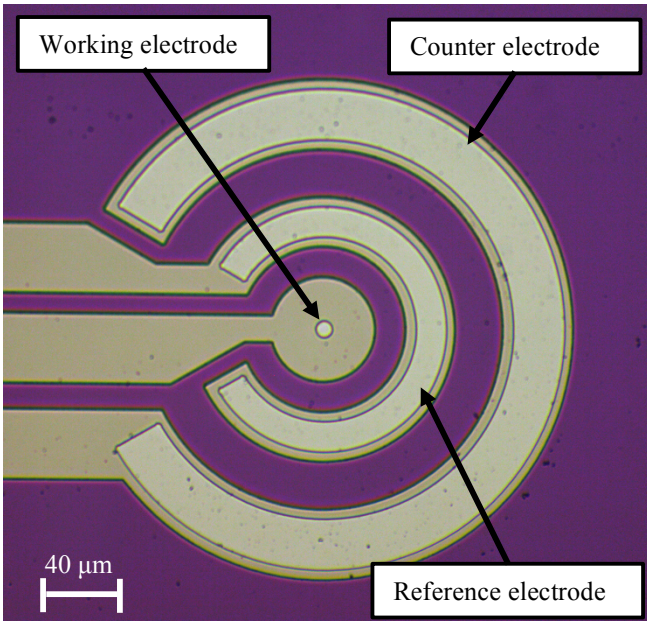

Fig. 8. Photomicrograph of the on-chip three electrode system

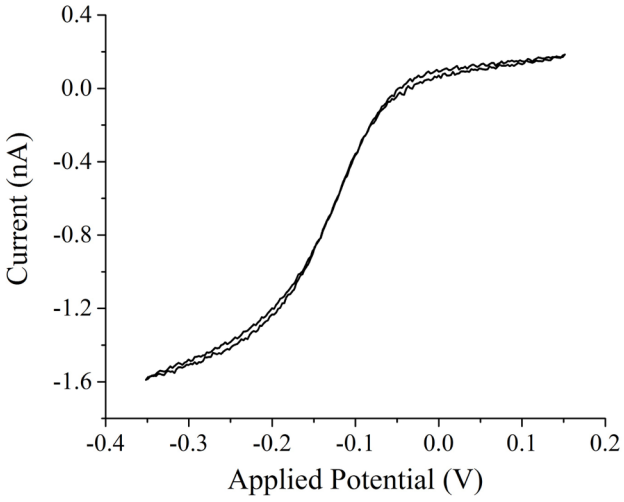

Fig. 9. Cyclic voltammogram of the reduction of ferricyanide in KCl at 200 mVs^{-1} in recorded using 5 µm radius platinum electrode, packaged.

VI. Conclusions

This paper has demonstrated a low-cost sensor packaging system, based on a DLP projector. This enables digitally-created patterns to be projected onto photo-curable resin, resulting in a versatile and simple process. The versatility of this was shown through production of a variety of shapes and channels, including the creation of a simple microfluidic system. The resolution and curing rate of the resin was then quantified.

TABLE III. MEASURED BOND RESISTANCES BEFORE AND AFTER PACKAGING FOR THREE TEST STRUCTURE CHIPS

	Average electrical resistance of wire bonds (Ω), errors ± 1 SD (Ω) (n = 4)		
	Chip 1	**Chip 2**	**Chip 3**
Before dispensing resin	9.8 ± 4.3	12.2 ± 2.1	12.6 ± 0.4
After packaging and cleaning	9.8 ± 3.9	12.3 ± 1	12 ± 1

TABLE IV. MEASURED SILICON OXIDE THICKNESS BEFORE AND AFTER PACKAGING FOR THREE TEST STRUCTURE CHIPS

	Average thickness of the exposed SiO2 layer, errors ± 1 SD (nm) (n = 5)		
	Chip 1	**Chip 2**	**Chip 3**
Before dispensing resin	470 ± 3	472 ± 3	471 ± 1
After packaging and cleaning	475 ± 2	473 ± 3	476 ± 2

The packaging process was also validated using dedicated test structures and was confirmed to: not affect the wire bond stability, not obscure the sensing surface with residue, and successfully insulate in a liquid environment. Finally an electrochemical sensor was packaged and a well-established redox couple measured. The current obtained closely matched that theoretically predicted, suggesting the sensor is functioning as expected. This presented system also facilitates rapid-prototyping, and the potential to combine this packaging technique with 3D printing expands the possible applications achievable with this system.

ACKNOWLEDGMENT

We would like to acknowledge the financial support of EPSRC (EP/K034510/1) IMPACT programme grant

REFERENCES

[1] PJ Hesketh and X Lin, "Packaging of Biomolecular and Chemical Microsensors," in *Nano-Bio-Electronic, Photonic and MEMs Packaging*, pp. 565 – 611, eds. CP Wong, KS Moon, and Y Li, 2010.

[2] B. Srinivasan and S. Tung, "Development and Applications of Portable Biosensors," *Journal of Laboratory Automation*, vol. 20, no. 4, pp. 365–389, 2015.

[3] C Cotofana, A Bossche, P Kaldenberg, and J Mollinger, "Low-cost plastic sensor packaging using the open-window package concept," *Sensors and Actuators A: Physical*, vol. 67, no. 1, pp. 185–190, 1998.

[4] Y. Qin, M. M. Howlader, J. M. Deen, Y. M. Haddara, and R. P. Selvaganapathy, "Polymer integration for packaging of implantable sensors," *Sensors and Actuators B: Chemical*, vol. 202, pp. 758–778, 2014

[5] A Cavallini, TR Jost, and SS Ghoreishizadeh, "A Subcutaneous Biochip for Remote Monitoring of Human Metabolism: packaging and biocompatibility assessment," *IEEE Sensors*, vol. 15, no. 1, pp. 417 – 424, 2015.

[6] D Welch and JB Christen, "CMOS biosensor system for on-chip cell culture with read-out circuitry and microfluidic packaging," *2012 Annual International Conference of the IEEE Engineering in Medicine and Biology Society (EMBC),* 2012.

[7] T Datta-Chaudhuri and P Abshire, "System-on-chip considerations for CMOS fluidic and biointerface applications," *2014 IEEE International Symposium on Circuits and Systems (ISCAS),* 2014.

[8] D Mark, S Haeberle, G Roth, F von Stetten, and R Zengerle, "Microfluidic lab-on-a-chip platforms: requirements, characteristics and applications", *Chemical Society Reviews*, vol. 39, 2010.

[9] S Haeberle and R Zengerle, "Microfluidic platforms for lab-on-a-chip applications", *Lab on a Chip*, vol. 7, pp. 1094 – 1110, 2007.

[10] S Sharma, J Zapatero-Rodríguez, and P Estrela, "Point-of-care diagnostics in low resource settings: present status and future role of microfluidics," *Biosensors*, vol. 5, no. 3, pp. 577 – 601, 2015.

[11] A Bratov, J Mun, C Dominguez, and J Bartroli, "Photocurable polymers applied as encapsulating materials for ISFET production," *Sensors and Actuators B: Chemical*, vol. 25, no. 1 – 3, pp. 823 – 825, 1995.

[12] V Mokkapati, O Bethge, R Hainberger, and H Brueckl, "Microfluidic chips fabrication from UV curable adhesives for heterogeneous integration," *IEEE 62nd Electronic Components and Technology Conference (ECTC)*, pp. 1965–1969, 2012.

[13] E O Blair, A Buchoux, A Tsiamis, C Dunare, J K R Marland, J G Terry, S Smith, and A J Walton, "Test Structures for the Characterisation of Sensor Packaging Technology," *IEEE 2017 International Conference for Microelectronic Test Structures*, Grenoble

[14] S J Konopka and B McDuffie, "Diffusion Coefficients of Ferri- and Ferrocyanide Ions in Aqueous Media, Using Twin-Electrode Thin-Layer Electrochemistry", *Analytical Chemistry*, vol. 42, no. 14, pp. 1741 – 1746, 1970.